Pressurized Formic Acid Dehydrogenation: An Entropic Spring Replaces Hydrogen Compression Cost

SCHOLARONE™
Manuscripts

ARTICLE

Pressurized Formic Acid Dehydrogenation: An Entropic Spring Replaces Hydrogen Compression Cost

Van K. Do[a], Nicolas Alfonso Vargas[a], Anthony J. Chavez[a], Long Zhang[a], Valeriy Cherepakhin[a], Zhiyao Lu[a], Robert P. Currier[b], Pavel A. Dub[b], John C. Gordon[c], and Travis J. Williams*[a]

Formic acid is unique among liquid organic hydrogen carriers (LOHCs), because its dehydrogenation is highly entropically driven. This enables the evolution of high-pressure hydrogen at mild temperatures that is difficult to achieve with other LOHCs, conceptually by releasing the "spring" of energy stored entropically in the liquid carrier. Applications calling for hydrogen-on-demand, such as vehicle filling, require pressurized H_2. Hydrogen compression dominates the cost for such applications, yet there are very few reports of selective, catalytic dehydrogenation of formic acid at elevated pressure. Herein, we show that homogenous catalysts with various ligand frameworks, including Noyori-type tridentate (PNP, SNS, SNP, SNPO), bidentate chelates (pyridyl)NHC, (pyridyl)phosphine, (pyridyl)sulfonamide, and their metallic precursors, are suitable catalysts for the dehydrogenation of neat formic acid under self-pressurizing conditions. Quite surprisingly, we discovered that their structural differences can be related to performance differences in their respective structural families, with some tolerant or intolerant of pressure and others that are significantly advantaged by pressurized conditions. We further find important roles for H_2 and CO in catalyst activation and speciation. In fact, for certain systems, CO behaves as a healing reagent when trapped in a pressurizing reactor system, enabling extended life from systems that would be otherwise deactivated.

Introduction

The production of hydrogen gas on demand is an enabling technology for the widespread deployment of hydrogen fuel cell vehicles. One approach to providing H_2 on demand is to release it catalytically from a liquid organic hydrogen carrier (LOHC), provided that the economics of such a system can overcome the costs of pressurizing and delivering the gas. Gas compression contributes 49% to 83% of the total refueling cost for light-duty and heavy-duty vehicles, respectively, in US retail cases.[1] Thus, the ability to produce *pressurized* H_2 on demand reduces the cost of H_2 in vehicle refueling. Yet, to our view, most catalyst development work on LOHC dehydrogenation has been under ambient pressure conditions.

Formic acid (FA, available from biomass fermentation or CO_2 electrolysis), is a low cost, sustainable hydrogen carrier with desirable volumetric density (1.22 g/mL) and H_2 content (4.4 wt %).[2, 3] Its dehydrogenation is significantly entropically driven, with $\Delta_r H^o$ = +7.4 kcal/mol and $\Delta_r S^o$ = +51 cal/mol·K, so entropic

energy released upon dehydrogenation serves as a type of spring, capable of delivering compressed hydrogen without the cost of compression. Self-pressurization of FA or alcohol dehydrogenation creates a unique environment for catalysis, where H_2, CO_2, and/or CO can govern catalyst initiation (e.g. in-situ catalyst synthesis), speciation, and decomposition. While carbonylation is a known poisoning pathway in many cases,[4, 5] we find that it can be essential to catalyst activation in others: for example, CO can play a healing role, extending the life of systems that would be deactivated without it. Despite these key advantages, we know of no broad studies of how closed-reactor conditions impact dehydrogenation catalysis;[5] the healing role of CO has been missed; and there are not generalizations for when this behavior might be expected or what the role of pressurization might have in directing it.

Hydrogen release from FA has been studied extensively in homogeneous and heterogeneous systems based on precious (Ir,[6, 7, 8] Ru,[8, 9, 10] Pd,[11, 12] and Au[13, 14]) and non-precious (Fe[15, 16] and Mn[17, 18]) metal catalysts, but we see only a few systems that are known to produce pressurized products while maintaining catalytic reactivity and selectivity.[19-24] Pioneering work by Fellay et al. described one of the first examples of high-pressure dehydrogenation of aqueous formic acid using a ruthenium catalyst.[23, 24] Since then, several groups have reported similar findings,[19-22] however, industrially relevant turnover frequencies (TOF) and turnover numbers (TON) have not been achieved using neat formic acid. Most recently, Milstein recently reported a ruthenium PNP pincer catalyst for the

a.Loker Hydrocarbon Research Institute, Wrigley Institute for Environmental Studies, and Department of Chemistry, University of Southern California, Los Angeles, California, 90089, United States.
b Chemistry Division, Los Alamos National Laboratory, Los Alamos, New Mexico 87545, United States.
c National Security Education Center (NSEC), Los Alamos National Laboratory, Los Alamos, New Mexico 87545, United States

dehydrogenation of neat FA, demonstrating the catalyst's tolerance of headspace H_2/CO_2 pressure (10-100 bar).[25]

We provide here the first general study of how FA dehydrogenation catalysts respond to self-pressurizing conditions. We demonstrate a broad survey of activity and stability of catalysts in both ambient and pressurized reaction conditions and find striking reactivity improvements for some catalysts when pressurized. We ultimately show how such improvements are realized, sometimes by transforming a monomeric catalyst into a two-metal pseudo-pincer type species upon carbonylation.

EXPERIMENTAL

Materials and Methods. All dehydrogenation experiments were set up and performed under inert atmosphere (N_2 gas) using standard Schlenk technique or a N_2-filled glovebox. Formic acid (BTC Beantown Chemicals, 97%), sodium formate (Sigma Aldrich, 97%), IrCl(COD) dimer (Chem-Impex Int'l Inc., >98%), Ru(p-Cymene)Cl_2 dimer (Strem Chemicals, 98%), Rh(CO)$_2$Cl dimer (Strem Chemicals, 97%), Rh(Cl)(COD) dimer (TCI Chemicals, 98%), Cp*IrCl$_2$ dimer (Combi Blocks Inc., 98%), Crabtree's catalyst (Alfa Aesar, 99%), Shvo's catalyst (Strem Chemicals, 98%), Gusev's catalyst (Sigma Aldrich, 97%), Ru-MACHO (Strem chemicals, 98%), Ru-MACHO-BH (Strem chemicals, 98%), carbonylchlorohydrido[bis(2-di-i-propylphosphinoethyl)amine]ruthenium(II) (Strem chemicals, 97%) were used as received without further purification. [RuCl(η^6-cymene)((2-pyridyl)$CH_2P^tBu_2$)]OTf, [Ir(κ^2-C,N-Mes)(CO)$_2$]OTf, [Ir(cod)(κ^2-C,N-Me)]OTf, Ru(PNS^{Me})(H$_2$) **5**, Ir(NNTos) **19**, Ir(NNTos) **20**, Ru(PNS^{Me})(Cl$_2$) were synthesized following reported literature procedures.[6, 26-30] All air and moisture sensitive procedures were carried out either in a Vacuum Atmosphere glovebox under nitrogen (2-10 ppm O_2 for all manipulations) or using standard Schlenk techniques under nitrogen. Ambient gas products are collected in a eudiometer by water displacement and pressurized gas products are quantified in a 125 mL non-stirred Parr reactor via a pressure gauge (0-200 bar).

General procedure.

1. Ambient pressure conditions: All catalysts in this study were stored in the glovebox under nitrogen, and glassware used (round bottom flasks, stir bars, water condensers, etc.) was oven dried prior to use. In the glovebox, catalyst (7.95 mmol) and sodium formate (1.20 g) were weighed out and added to a round bottom flask equipped with a magnetic stir bar. Formic acid (3.00 mL, 79.5 mmol) was measured out and added to the same flask via a syringe. The flask was connected to a water condenser with a Tygon tubing. The other end of the tubing was submerged in an inverted graduated cylinder (eudiometer). Oil bath temperature was set to 110 °C. Evolved gas volume was recorded by water eudiometry.

2. Self-pressurized conditions: In the glovebox under nitrogen, catalyst (7.95 mmol) and sodium formate (1.20 g) were weighted out and added to an 8-dram vial equipped with a magnetic stir bar. Formic acid (3.00 mL, 79.5 mmol) was measured out and added to the same vial via a syringe. The solution was transferred and sealed in a 125 mL Parr apparatus. The internal temperature of the reactor was set at 110 °C (± 5 °C) and monitored closely via a thermocouple to minimize temperature difference between the oil bath and the reaction temperature. Evolved gas pressure was monitored via the reactor's pressure gauge.

3. H_2/CO Gas Pre-Treatment: Similar procedure to 3.2.2., except the reaction was charged with either H_2 or CO to the desired pressure at room temperature and let stir at 110 °C. Evolved gas pressure was monitored via the reactor's pressure gauge.

RESULTS AND DISCUSSION

Catalysts for FA Dehydrogenation at Ambient and Self-pressurizing Conditions.

Table 1. Dehydrogenation of neat FA at ambient pressure versus under pressurized operation.

Entry[a]	Catalyst precursor	Conversion at ambient pressure[c]	Conversion in pressurized vessel (Evolved pressure in bar)[d]
1a	**1**	6 %	42 % (16)
1b[b]	**1**	6 %	82 % (31)
2a	**2**	8 %	29 % (11)
2b[b]	**2**	9 %	58 % (22)
3	**3**	9 %	71 % (27)
4a	**4**	2 %	40 % (15)
4b[b]	**4**	3 %	79 % (30)
5	**5**	3 %	79 % (30)
6a	**6**	9 %	84 % (32)
6b[b]	**6**	3 %	84 % (32)
7	**7**	63 %	74 % (28)
8	**8**	10 %	32 % (12)
9a	**9**	12 %	86 % (33)
9b	**9-CO**	35 %	92 % (35)
10	**10**	6 %	55 % (21)
11	**11**	>99 %	100 % (38)
12	**12**	>99 %	100 % (38)
13	**13**	0 %	32 % (12)
14	**14**	1 %	74 % (28)
15	**15**	2 %	16 % (6)
16	**16**	3 %	16 % (6)
17	**17**	23 %	42 % (16)
18	**18**	3 %	32 % (12)
19[e]	**19**	>99 %	100 % (38)
20	**20**	33 %	100 % (38)
21	**21**	5 %	84 % (32)

[a]Conditions: catalyst (0.00795 mmol, 100 ppm), FA (3.0 mL, 79.5 mmol), and NaO$_2$CH (1.2 g, 17.6 mmol) at 110 °C. [b]Pre-activation with 2.0 eq. of KO^{t}Bu in toluene (0.5 mL) at 25 °C. [c]FA conversion in opened system. [d]FA conversion in closed system (3.0 ml) calculated based on full conversion (38 bar) of entry 11. [e]Reported best yield of 3 replications.
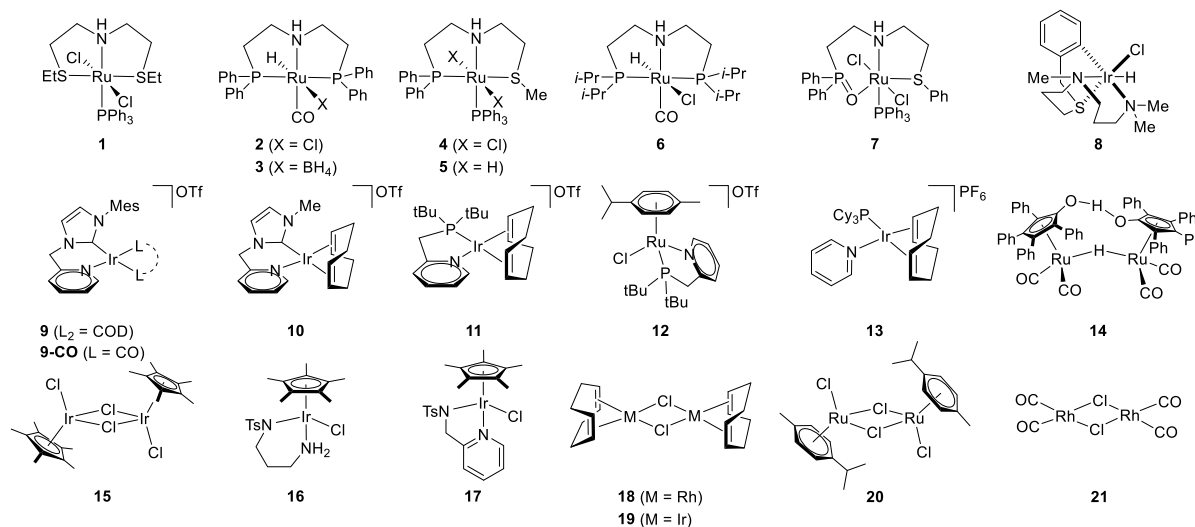
ARTICLE

Fig. 1 Late-transition metal complexes tested for formic acid dehydrogenation in this study.

We surveyed a wide range of complexes that generally fit into four classes: (1) Noyori-type tridentate complexes **1**-**8**, (2) bidentate chelates complexes **9**-**12** and their analog **13**, (3) cyclopentadienyl piano stools complexes **14**-**17**, and (4) metal precursors for the ligated complexes **18**-**21** (Figure 1). Each was examined in FA dehydrogenation both under ambient pressure and self-pressurizing conditions to determine catalyst activity and efficiency (Table 1). While every complex is different under these conditions, some generalizations of each class can be identified.

Table 1 shows the results of FA dehydrogenation conducted under both ambient and self-pressurizing conditions. *All twenty-one complexes react with FA at a higher rate when pressurized than they do at ambient pressure*, each without detectable reversibility (see Figure S4-S30 for time course data). The overall improvement in conversion efficiency varied between a minimum of +13% (entries 15 and 16) and a maximum of +72% (entry 14) as conditions changed from open to closed vessels. For example, mildly active complex **20** at ambient pressure promoted complete conversion when in a closed system (entry 20). Perhaps most startling, complexes **1**-**6**, **8**, **10**, **13**, and **21** exhibit little reactivity at ambient pressure but are dramatically more reactive under self-pressurizing conditions. An exception was observed in complex **7**[26, 27, 28] which has competitive reaction conversion at both ambient and pressurized conditions (Figure S15).

Complexes **1**-**8** in the well-studied Noyori-type tridentate family, generally featuring M(PNL) (L = PPh$_2$, P(^{i}Pr)$_2$, S(CH$_3$)$_2$) structures, tend to have *lower reactivity* than other catalysts at ambient pressure, giving conversions between 2% and 10%; but

they are the *highly impacted* by pressurization relative to the other classes, reaching conversions from 58% to 84% under self-pressurizing conditions. Complex **7** is a notable exception to both of these generalizations, possibly owing to the semi-lability of its phosphine oxide and the lower hydricity of its active form; whereas in an ester hydrogenation reaction, complex **7** is one order of magnitude less efficient than complex **4**.[26] Often, complexes in this class require pre-activation via hydrodechlorination with KOH or KO^{t}Bu to generate their active hydride forms.[9, 26, 31, 32, 33] Nevertheless, under self-pressurizing conditions, there was an increase in conversion from 21% (entry 2a) to 75% (entry 6a) without such pre-activation. For example, self-pressurization enables complex **4** (entry 4b) to achieve 79% conversion, comparable to its activated dihydride derivative (entry 5, 79%). Complex **6** can be initiated under pressurizing conditions without any base to convert 84% FA, while at ambient pressure only 3.4% FA is converted, even if the catalyst is activated with KO^{t}Bu. This dramatic enhancement of reactivity upon pressurization suggests that one of the reaction products, like H$_2$ or CO, is necessary to enable or maintain catalytic activity. Hydrogenation is known to activate amine-containing Noyori-type complexes such as **1**-**6** in the presence of base,[9, 31, 32, 33] which is a possible explanation. Further, we observe that thermal decarbonylation of FA is possible at our operating temperature (vide infra). We expect that the trace CO generated through this pathway is oxidized rapidly by the catalyst, but that its continued supply installs or maintains a CO ligand on the catalyst.

Bidentate chelate complexes **9-CO**, **11**,[6, 29, 34, 35, 36] and **12** are the *most reactive* precursors that we encountered at ambient
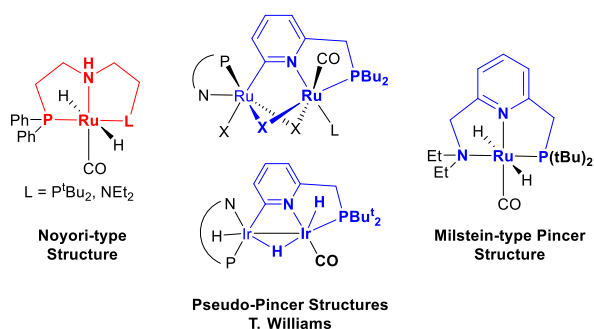
ARTICLE

Fig. 2 Structural analogy between the common Noyori-type, Milstein-type pincer and our pseudo-pincer active catalytic species.

pressure.[37] Complex **11** exhibits the highest rate of the entire library, where in 79.5 mmol of FA were fully converted within 1.2 hours. We found these complexes to be pressure-tolerant, but with little enhancement in reactivity because of their high baseline efficiency at ambient pressure. We believe the unique reactivity of these complexes to be a function of a novel self-assembly pathway: these convert to two-metal pseudo-pincer structures in the presence of a CO (isolated and characterized from reaction mixtures), exemplified by cases of our (pyridyl)phosphine ligand bound to ruthenium and iridium (Figure 2).[6, 37] These pathways are available at ambient pressure either from FA or an alcohol. [6, 29, 34, 35, 36] The resulting bimetallic complexes have high activity and stability at ambient or elevated pressure. The active complexes have structural homology with some prolific Noyori-type and Milstein-type pincer complexes, where one arm of the tridentate ligand is replaced by the second metal.[38, 39]

Carbene-ligated compound **10** in this class lacks the reactivity of **9-CO**, **11**, or **12**. While the reactivity of carbene-ligated systems **9-CO** and **10** should be different than their phosphine-ligated congeners **11** and **12**, it is surprising that **10** does not react analogously to **9-CO** under pressurized conditions, especially whereas **9-CO** is prepared from its cyclooctadiene-ligated precursor **9** at ambient pressure (vide infra). Crabtree's catalyst **13** also exhibits low reactivity compared to its bidentate analog **11**. We infer that tethering the pyridine and phosphine groups is important for proper catalyst self-assembly.

Piano stool Cp*Ir complexes **15-17** are not very efficient in this study, although they are *moderately aided* by pressure. Complexes **16** and **17** have been known to have excellent reactivity in alcohol dehydrogenation,[30, 39] but their activity towards FA is moderate, respectively 16% and 42% conversion under pressurizing conditions. Notably, Shvo's cyclopentadienone-ligated catalyst **14** is much more reactive

than Cp*Ir systems under pressurizing condition. The Shvo system is known to rest in its dimeric form **14** in the presence of H_2,[40, 41, 42] so we reason that the availability of CO to trap the system's oxidized monomer and prevent formation of **14** could account for its rate advantage upon pressurization, because it is known that H_2 pressure will drive the system back to dimer **14**.[41, 42, 43]

While several of the ligated species in Table 1 are efficient catalysts—they were designed as such—we were surprised to find that their synthetic precursors **18-21**[6, 36, 37] have reactivity that rivals their ligated congeners. We find, however, that unlike the ligated congeners, the unligated precursors seem to deactivate easily. Overall, one piece of traditional wisdom that seems to be preserved is that ligated complexes tend to have good stability, sometimes at the cost of reaction rate. For example, we had difficulty replicating entries **18**-**21** whilst other entries were very reliable. Apparently, these more naked species tend to react quickly, yet the reactivity is short-lived and difficult to replicate.

Impact of Applied H_2 and CO

Whereas many of the complexes we screened are more productive under self-pressurizing conditions, we conclude that initially formed products, probably CO and H_2, are involved in activating the precatalysts[5, 37] and healing the active catalyst by preempting deactivation processes. We propose that these processes could be emulated by adding CO or H_2 at the outset of the reaction. To test this, reactions involving four catalyst precursors, **5**, **10**, **14**, and **15**, were examined representing the 3 respective classes of ligated precatalysts that benefitted significantly from self-pressurizing conditions. These were alternatively pretreated with H_2 or CO in FA and their catalytic activity was evaluated (Figure 3).

Neither H_2 (green triangles) nor CO (orange circles) uniformly improved catalytic activity over baseline (black squares) of every catalyst tested. While complexes **15** and **10** benefit respectively from H_2 and CO pretreatment, other combinations of catalyst and treatment did not significantly improve reactivity: there is not a generalization that explains why these four complexes are accelerated by pressure. By contrast, both **10** and **5** are deactivated by H_2 pretreatment. In the case of the Shvo system **14**, H_2 pressure slows the reaction but did not affect maximum total pressure (27-28 bar), consistent with the above proposal of dimer formation.

Notably, after **10** was pretreated with CO, the activity was significantly improved, reaching 89% conversion in five hours, surpassing its carbonylated homolog **9-CO**. This is an interesting contrast to the relatively low reactivity of **9** under self-pressurizing conditions (vide supra): apparently insufficient CO
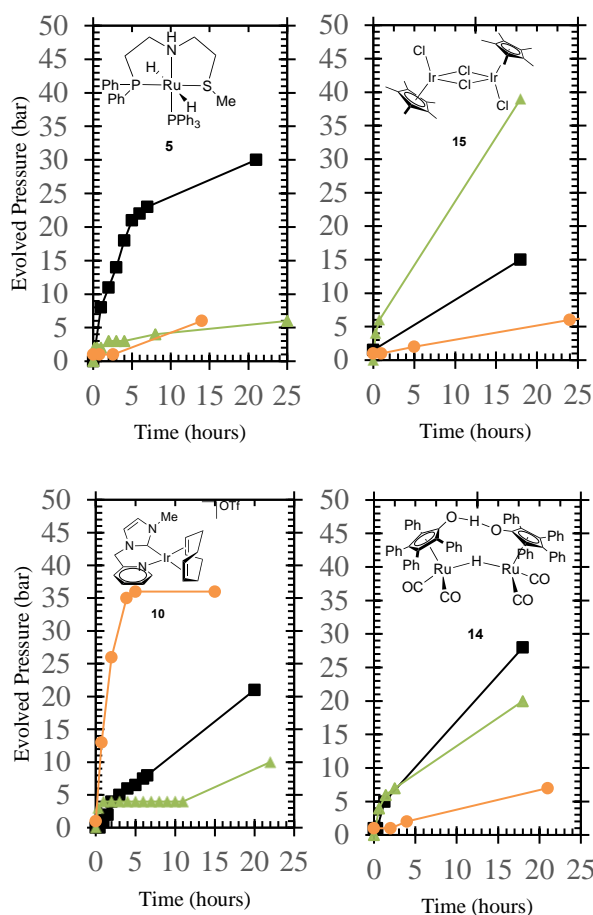
Fig. 3 Pressurized dehydrogenations of FA: control (black squares), pretreated with 8 bar of H_2 (green triangles), (orange circles) pretreated with 1 bar of CO following by N_2 purging. Top left. complex **5**; Top right. complex **15**; Bottom left. complex **10**; Bottom right. complex **14**.

is generated by formic acid dehydrogenation to realize the full benefit of carbonylation. Also very interesting about this catalyst system is that at ambient pressure, reactivity slows after about 3 minutes, which is not observed under pressurizing conditions. We view this as evidence that CO heals the catalyst and maintains fast kinetics when it does not have the opportunity to escape the reactor. Despite numerous cases of catalyst poisoning by metal carbonylation,[4, 5] complexes **9-CO** and **10** exhibit the opposite effect: in the absence of CO, **10** has low activity for FA decomposition, but when CO is introduced, either by self-generation or pretreatment, complex **10** performed ca. three times (added CO, Figure 3) to four times (self-generated CO, Table 1, entry 9b) better.

Whereas CO is essential to the activation of these catalyst systems, it must be available in the reactor, although it is not detected in the product stream of FA dehydrogenation as reported in many studies from our lab and others.[5] Although

Scheme 1. Synthesis and molecular structures of **9-CO** and **11-CO**.[a]
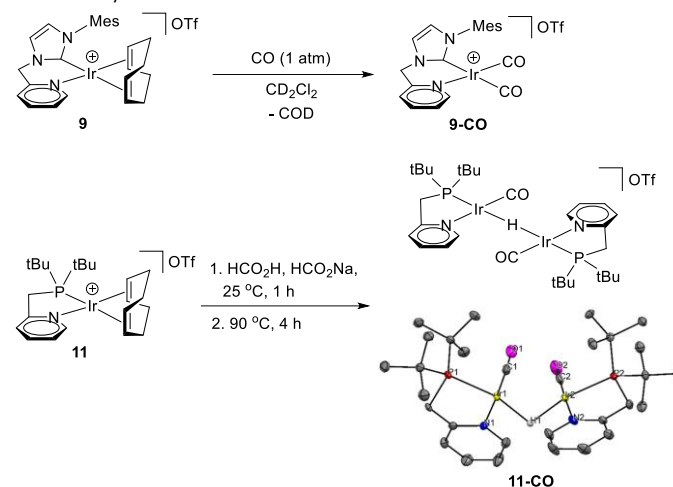
[a]CCDC 2142637 contains supplementary crystallographic data for **11-CO**.

there has not been a full explanation of this, we believe that formation of CO occurs thermally,[44, 45] possibly catalyzed by traces of metals in the reactor vessel, and that CO is oxidized rapidly by the catalyst in our conditions. We tested these ideas with two experiments: (1) when the reaction was run with precursor **11** under pressurizing conditions and utilizing rapid heating, the reactor reaching over 129 ^oC at times, we detected CO concentration up to 0.63%, concurrent with fast H_2 generation (107 L/h). No CO (< 10 ppm) is observed under analogous conditions below 100 ^oC. This suggests that thermal decarbonylation of FA can produce significant CO concentration if not controlled;[44, 45] (2) In an aqueous methanol photodehydrogenation experiment (Table S9), 6% of CO was generated in the absence of catalyst **10**, whereas none can be detected when **10** is present. Complex **10** was chosen for this experiment for its relatively slow reactivity in FA dehydrogenation, thus to allow longer life and easier observation of C1 intermediates. We infer from this observation that, when CO is produced by a non-catalytic reaction, the presence of an appropriate metal complex will reform the CO efficiently: CO is available, but not detectable. We suspect that this is a general feature of homogeneous catalysts for formic acid dehydrogenation that has not previously been described.

Whereas CO is vital to the initiation and speciation of some catalysts, we attempted to prepare species by independent synthesis that could be responsible for the observations. Upon treating **10** with 1 atm CO, we found that **10-CO** was not stable to isolation. Treatment of **11** with CO results in a broad diversity of structures, which we have previously reported.[29] While these systems failed, the clean carbonylated species **9** readily yielded **9-CO** upon carbonylation.[29] We measured the kinetics of dehydrogenation with **9** and **9-CO** at ambient pressure to test the hypothesis that CO plays a role in precatalyst activation. At ambient pressure, complex **9-CO** dehydrogenates FA faster
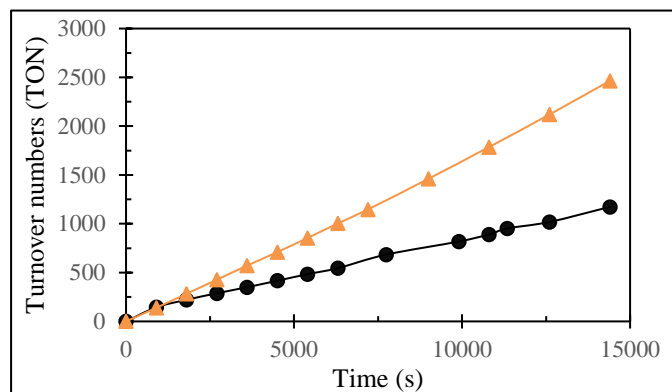
ARTICLE

Fig. 4 Kinetic profile of formic acid dehydrogenation by **9** (black circles) and **9-CO** (orange triangles). Conditions: Ir complex (0.00795 mmol, 100 ppm), FA (3.0 mL, 79.5 mmol), and NaO_2CH (1.2g, 17.6 mmol) at 110 °C.

Fig. 5 Gas evolution of FA dehydrogenation by complex **9** (orange) and **9-CO** (blue) over time upon treatment of 0 bar CO – diamond; 2 bar CO – triangles; 8 bar CO – circles.

than precursor **9** (Figure 4): both show saturation catalysis through a 4-hour experiment, with **9-CO** at 24.6% conversion ($16.5(1) \times 10^{-2}$ TOF) relative to **9** at 11.7% conversion ($8.3(1) \times 10^{-2}$ TOF). These data indicate an important role for CO in the reactivity of catalyst **9**.

Further investigation of CO pressure revealed the expected inhibitory role at higher loading (Figure 5 and S31). At low concentration of CO either from FA decomposition or treatment with 2 bar of CO, **9** initiates at a faster rate than in the absence of CO. By contrast, under 8 bar of CO, we observe slower conversion of the catalytic reaction following rapid initiation as shown in Figure 5. As expected, **9-CO** performed substantially similar to **9** when **9** is treated with 2 bar CO, but like **9**, **9-CO** exhibits inhibited rate when 8 bar CO is applied.

While seeking to understand the activation pathway of our most active precursor **11**, a stable species **11-CO** was isolated from a FA dehydrogenation reaction at ambient pressure (Scheme 1). Complex **11-CO** was characterized by ^{1}H, ^{13}C, ^{19}F, and ^{31}P NMR spectroscopy and its molecular structure was established by single-crystal X-ray diffraction. Formation of carbonyl complex **11-CO** under these conditions is a remarkable development, since FA dehydrogenation catalyzed by **11** is known to produce no free CO gas (< 10 ppm) and returns non-carbonylated catalytic species when operated at 90 °C.[6] This teaches us that at sufficient temperature and pressure, the previously characterized resting species from the **11**-catalyzed dehydrogenation of FA can be further converted into a carbonylated system **11-CO**. Again, we see that while FA decarbonylation happens during catalysis, CO is reformed rapidly to products and remains undetectable in the product stream.
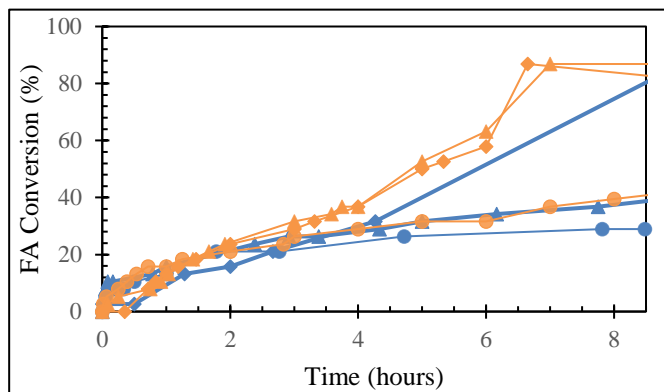
Regeneration, Activity, and Selectivity of 11 in High Pressure Gas Stream Production.

To the best of our knowledge, precursor **11** continues to demonstrate comparable or superior activity to all known homogeneous systems for dehydrogenation of neat FA (Figure S4). It also provides excellent stability, longevity (TON > 2 million) and selectivity[6] ($H_2:CO_2$ 1:1, CO < 10 ppm). We thus scaled this system to generate a pressurized product stream (> 103 bar) while demonstrating longevity and exceptional kinetics. To acquire high resolution data, we used a 600 mL stirred pressure vessel equipped with an internal temperature probe and a pressure transducer (see Supporting Information). We report volumetric flow rate (standardized to 1 atm at 0 °C) in units of liters per hour (L/hr corrected to ambient conditions) for all H_2 evolution rates.

A 20-cycle pressure experiment was accomplished using 99.6 mg (145 µmol) of complex **11** and 20 g (294 mmol) of sodium formate co-catalyst in 55 mL of FA (Figure 6). During each cycle, ca. 50 mL of FA was added (1 L, 17.9 mol over 20 cycles), the reactor was sealed and heated to 120 °C, then the pressure was allowed to build to 117 bar (approximately 25 L of H_2). Once the desired pressure was achieved, the reaction was quenched by rapid cooling in a dry-ice bath and then depressurized to repeat the cycle. The reaction rate in the form of evolved H_2 per hour is plotted in Figure 6. This experiment illustrates that once pre-catalyst **11** is initiated, there is no detectable deactivation of the catalyst through 200,000 turnovers as evidenced by the consistently high peak reaction rates, varying only due to concentration differences between individual experiments. Cycle 4 demonstrated that when allowed to run near dryness, the peak reaction rate exceeded 160 L/hr, corresponding to a TOF of nearly 50,000 hr^{-1}.
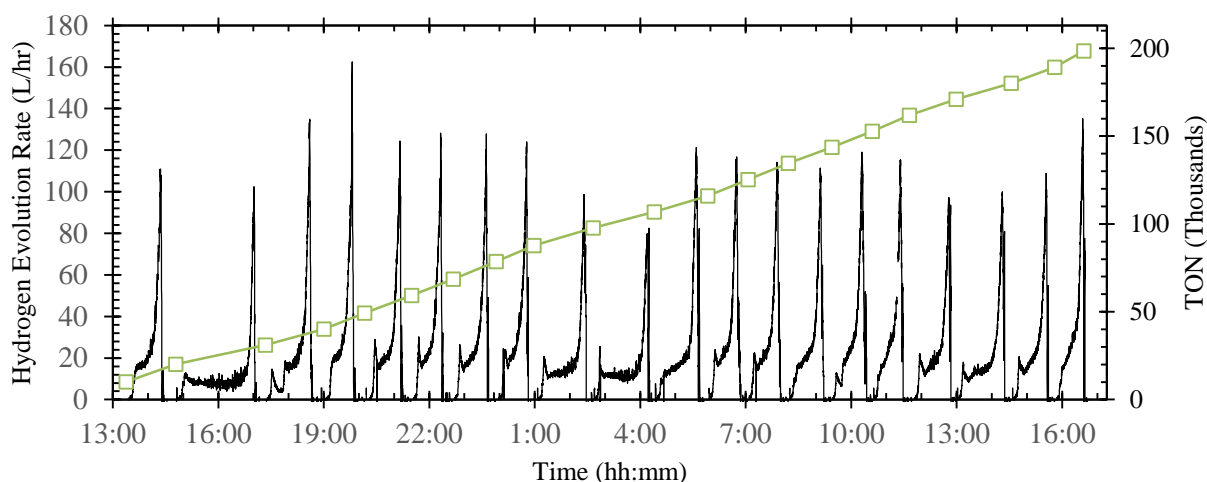
Fig. 6 Catalyst recycling study in FA dehydrogenation by complex **11**.

Conclusions

Among a library of late-transition metal complexes, we found that *in every case studied* the dehydrogenation of neat FA is more productive under self-pressurizing reaction conditions. This is a stunning outcome, whereas the cost of hydrogen provided for retail vehicle filling is dominated by the cost of compressing the gas yet we have few detailed and broad-based studies that show how pressure evolution impacts the efficacy of homogeneous FA dehydrogenation catalysts. We grouped catalysts for neat FA dehydrogenation into four general classes, pincers, bidentate chelates, piano stool complexes, and metal precursors. Each structural class uniquely responds to pressurized condition. The bidentate chelates excel beyond others, which we attribute to a transformation from monomers to two-metal pseudo-pincer complexes in which the second metal seems to impart special reactivity. We find an enabling role for CO and/or H_2 in a number of cases, typically impacting catalyst initiation (in-situ catalyst synthesis) and defining the course of catalyst speciation. This hypothesis is supported by previous studies[5, 37], namely, the observation and isolation of the carbonylation derivative of **11**, and the 3-fold increase in a healing process of **10** by CO. In addition, complex **11**, which exhibits exceptional catalytic activity, stability, and selectivity, supersedes existing systems in the production of a high-pressure product stream from neat FA dehydrogenation. This catalyst was used to convert over 1 L of formic acid into pressurized H_2/CO_2 product over the course of 30 hours, proving that the catalytic activity could be maintained at a high level for 200,000 turnovers at 117 bar without any loss of reactivity. Due to the favorable economics of producing H_2 at

pressure, fully automated H_2 generation using a continuous feed, stirred tank reactor will be developed to evaluate the ultimate longevity of the catalyst. This technology and the discovery of a detailed mechanism and speciation of **11** will be reported in future work.

Conflicts of interest

T.J.W. and Z.L. are founders of startup company, Catapower Inc., that is commercializing **10** for lactate synthesis. LANL (P.A.D.) commercialized complexes **4**, **7**, and **8**, which are available from STREM Chemicals. N. A. V. is a founder of a company, Solargonic LLC, that aims to commercialize liquid hydrogen carriers.

Funding Sources

Acknowledgements

Notes and references

1   Hydrogen Technologies R&D Overview, (Hydrogen program, accessed June 30, 2021) https://www.hydrogen.energy.gov/pdfs/review21/plenary7_stetson_2021_o.pdf.

2   Mazloomi, K.; Gomes, C., *Renew. Sust. Energ. Rev.*, 2012, **16**, 3024-3033.

3   Sponholz, P.; Mellmann, D.; Junge, H.; Beller, M., *ChemSusChem.*, 2013, **6**, 1172-1176.

4   Iguchi, M.; Onishi, N.; Himeda, Y.; and Kawanami, H., *ChemPhysChem*, 2019, **20**, 1296-1300.

5   Alfonso, N.; Do, V. K.; Chavez, A. J.; Chen, Y.; Williams, T. J., *Catal. Sci. Technol.*, 2021, **11**, 2361-2368.

6   Celaje, J. J. A.; Lu, Z.; Kedzie, E. A.; Terrile, N. J.; Lo, J. N.; Williams, T. J., *Nat. Commun.*, 2016, **7**, 11308.

7   Wang, Z.; Lu, S.-M.; Li, J.; Wang, J.; Li, C., *Chem. Eur. J.*, 2015, **21**, 12592-12595.

8   Siek, S.; Burks, D. B.; Gerlach, D. L.; Liang, G.; Tesh, J. M.; Thompson, C. R.; Qu, F.; Shankwitz, J. E.; Vasquez, R. M.; Chambers, N.; Szulczewski, G. J.; Grotjahn, D. B.; Webster, C. E., and Papish, E. T., *Organometallics*, 2017, **36**, 1091-1106.

9   Agapova, A.; Alberico, E.; Kammer, A.; Junge, H.; Beller, M., *ChemCatChem*, 2019, **11**, 1910-1914.

10   Thevenon, A.; Frost-Pennington, E.; Weijia, G.; Dalebrook, A. F.; Laurenczy, G., *ChemCatChem*, 2014, **6**, 3146-3152.

11   Qin, X.; Li, H.; Xie, S.; Li, K.; Jiang, T.; Ma, X.-Y.; Jiang, K.; Zhang, Q.; Terasaki, O.; Wu, Z.; Cai, W.-B., *ACS Catal.*, 2020, **10**, 3921-3932.

12   Zhong, H.; Iguchi, M.; Song, F.-Z.; Chatterjee, M.; Ishizaka, T.; Nagao, I.; Xu, Q.; Kawanami, H., *Sustain. Energy Fuels*, 2017, **1**, 1049-1055.

13   Huang, Y.; Zhou, X.; Yin, M.; Liu, C.; Xing, W., *Chem. Mater.*, 2010, **22**, 5122-5128.

14   Liu, Q.; Yang, X.; Huang, Y.; Xu, S.; Su, X.; Pan, X.; Xu, J.; Wang, A.; Liang, C.; Wang, X.; Zhang, T., *Energy Environ. Sci.*, 2015, **8**, 3204-3207.

15   Bielinski, E. A.; Lagaditis, P. O.; Zhang, Y.; Mercado, B. Q.; Würtele, C.; Bernskoetter, W. H.; Hazari, N.; Schneider, S., *J. Am. Chem. Soc.*, 2014, **136**, 10234-10237.

16   Léval, A.; Agapova, A.; Steinlechner, C.; Alberico, E.; Junge, H.; Beller, M., *Green Chem.*, 2020, **22**, 913-920.

17   Sun, Q.; Chen, B. W. J.; Wang, N.; He, Q.; Chang, A.; Yang, C.-M.; Asakura, H.; Tanaka, T.; Hülsey, M. J.; Wang, C.-H.; Yu, J.; Yan, N., *Angew. Chem. Int. Ed.*, 2020, **59**, 20183-20191.

18   Zell, T.; Butschke, B.; Ben-David, Y.; Milstein, D., *Chem. Eur. J.*, 2013, **19**, 8068-8072.

19   Himeda, Y., *Green Chemistry*, 2009, **11**, 2018-2022.

20   Manaka, Y.; Wang, W.-H.; Suna, Y.; Kambayashi, H.; Muckerman, J. T.; Fujita, E.; and Himeda, Y., *Catal. Sci. Technol.*, 2014, **4**, 34-37.

21   Iguchi, M.; Himeda, Y.; Manaka, Y.; and Kawanami, H., *ChemSusChem*, 2016, **9**, 2749-2753.

22   Iguchi, M.; Zhong, H.; Himeda, Y.; and H. Kawanami, *Chemistry – A European Journal*, 2017, **23**, 17788-17793.

23   Fellay, C.; Dyson, P. J.; and Laurenczy, C., *Angew. Chem. Int. Ed.*, 2008, **47**, 3966-3968.

24   Fellay, C., Yan, N., Dyson, P.J. and Laurenczy, G., *Chem. Eur. J.*, 2009, **15**, 3752-3760.

25   Kar, S.; Rauch, M.; Leitus, G.; Ben-David, Y.; Milstein, D., *Nat.*, 2021, **4**, 193-201.

26   Dub, P. A.; Batrice, R. J.; Gordon, J. C.; Scott, B. L.; Minko, Y.; Schmidt, J. G.; and Williams, R. F., *Org. Process Res. Dev.*, 2020, **24**, 415-442.

27   Dub, P. A.; Gordon, J. C. Polydentate Ligands and Their Complexes for Molecular Catalysis. U.S. Patent US 10550139 B2, February 4, 2020.

28   Dub, P. A.; Batrice, R. J.; Gordon, J. C. Synthesis of Fluoro Hemiacetals via Transition Metal-Catalyzed Fluoro Ester and Carboxamide Hydrogenation. U.S. Patent US 20200308089 A1, January 10, 2020.

29   Lu, Z.; Demianets, I.; Hamze, R.; Terrile, N. J.; Williams, T. J., *ACS Catal.*, 2016, **6**, 2014-2017.

30   Demianets, I.; Cherepakhin, V.; Maertens, A.; Lauridsen, P. J.; Mallikarjun Sharada, S.; Williams, T. J., *Polyhedron*, 2020, **182**, 114508.

31   Padmanaban, S.; Gunasekar, G. H.; Yoon, S., *Inorg. Chem.*, 2021, **60**, 6881-6888.

32   Dub, P. A., *Eur. J. Inorg. Chem.*, 2021, **2021**, 4884-4889.

33   Otsuka, T.; Ishii, A.; Dub, P. A.; and Ikariya, T., *J. Am. Chem. Soc.*, 2013, **135**, 9600-9603

34   Cherepakhin, V.; Williams, T. J., *ACS Catal.*, 2018, **8**, 3754-3763.

35   Lauridsen, P. J.; Lu, Z.; Celaje, J. J. A.; Kedzie, E. A. and Williams, T. J., *Dalton Trans.*, 2018, **47**, 13559-13564.

36   Lu, Z.; Cherepakhin, V.; Demianets, I.; Lauridsen, P. J.; and Williams, T. J., *ChemComm.*, 2018, **54**, 7711-7724.

37   Cherepakhin, V.; Williams, T. J., *ACS Catal.*, 2020, **10**, 56-65.

38   Gonçalves, T. P.; Huang, K.-W., *J. Am. Chem. Soc.*, 2017, **139**, 13442-13449.

39   Gunanathan, C.; Milstein, D., *Acc. Chem. Res.*, 2011, **44**, 588-602.

40   Nakamura, H.; Yoshida, M.; Matsunami, A.; Kuwata, S.; Kayaki, Y., *ChemComm*, 2021, **57** (45), 5534-5537.

41   Conley, B. L.; Pennington-Boggio, M. K.; Boz, E.; Williams, T. J., *Chem. Rev.*, 2010, **110**, 2294-2312.

42   Casey, C. P.; Johnson, J. B., *J. Am. Chem. Soc.*, 2005, **127**, 1883-1894.

43   Gusev, D. G., and Spasyuk, D. M., *ACS Catalysis*, 2018, **8**, 6851-6861.

44   Yu, J.; Savage, P. E., *Ind. Eng. Chem. Res.*, 1998, **37**, 2–10.

45   Akiya, N.; Savage, P., E. *AIChE J.*, 1998, **44**, 405–415.